JOURNAL OF CATALYSIS 42, 294–302 (1976)

Ultrahigh Magnetic Field Measurements of Nickel Crystallite Size Distributions

J. T. RICHARDSON AND P. DESAI

Department of Chemical Engineering, University of Houston, Houston, Texas 77004

Received November 11, 1975

Dispersed nickel supported on silica and alumina has been characterized with ultrahigh field magnetization measurements. A superconducting solenoid operable up to 100 kOe was used for this purpose. The samples were superparamagnetic so that the computation of crystallite size distributions from the magnetic data was possible. A computational technique was developed for this purpose and tests on model distributions carried out. Much better results were obtained than hitherto possible.

The catalysts, containing 40 wt% Ni, were initially bidisperse, with both low and high radii grouped distributions. Evidence for both crystallite migration in the case of the small particles and interparticle transport for the larger radii was detected. Measured and calculated surface areas were in agreement.

INTRODUCTION

Precise measurements of crystallite size distributions of supported metal catalysts are important for two reasons. The distribution is far more important with demanding or structure-sensitive reactions than the exposed surface area in establishing the catalytic activity (*1*). Secondly, dispersed catalysts deactivate by sintering. Discrimination between various sintering mechanisms may only be possible through analysis of changes in the distribution during crystallite growth (*2–4*).

X-ray diffraction and selective gas adsorption techniques give only average sizes and both require assumptions for the crystal shape and degree of support bonding (*5*). Small angle X-ray scattering may be utilized in certain cases to fit the parameters of assumed distributions (*6*). Transmission electron microscopy is direct, but involves the tedious examination of many specimens which are not necessarily truly representative of the sample (*5*). Furthermore, instrumental complications introduce inaccuracies in the case of very small crystallites (*7*).

Magnetic granulometry has for some time offered possibilities (*8*). Although limited to ferromagnetic metals, this method does have the advantage of potential *in situ* measurements, applicable to a wide class of industrially important catalysts. Selwood (*9*) has reviewed much of the work on nickel.

The technique is based on relationships in superparamagnetism. If a nickel crystallite is less than a single magnetic domain (300 Å) in size, then for a spherical radius r,

$$\frac{\sigma}{\sigma_\infty} = L(I_s H 4\pi r^3/3kT), \qquad (1)$$

where σ is the magnetization, σ_∞ the saturation magnetization, I_s the spontaneous magnetization, H the local magnetic field, T the temperature, k the Boltzmann constant and L the Langevin function. It is assumed that $\sigma_\infty = 4\pi r^3 I_s/3$

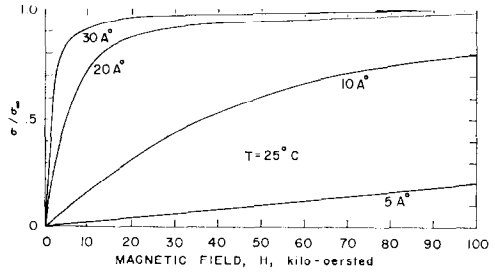

FIG. 1. Langevin function at 298°K for different sizes of nickel crystallites.

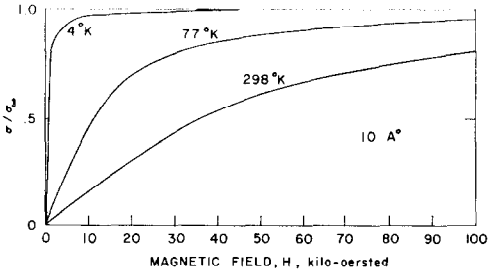

FIG. 3. Effect of temperature on the Langevin function of a 10 Å nickel crystallite.

and that I_s is independent of size. The validity of this assumption has been demonstrated by Abeledo and Selwood (*10*).

Figure 1 shows the calculated values of Eq. (1) at different magnetic fields and crystallite radii. In theory, the radius of the crystallite could be found by fitting σ versus H data to this function. However, serious problems arise in practice. The value of σ_∞ must first be obtained in order to establish the ordinate of Fig. 1. Most laboratory electromagnets are limited to 20 kOe where only crystallites with radii greater than about 20 Å approach saturation. It is usual to determine σ_∞ by extrapolation of $1/H$ plots to zero. The danger of this procedure is demonstrated in Fig. 2. Clearly, for radii less than 20 Å, linear extrapolations of data taken below 20 kOe result in large errors. The problem is usually circumvented, as shown in Fig. 3, by decreasing the temperature to 77 or 4.2°K, where more accurate extrapolations

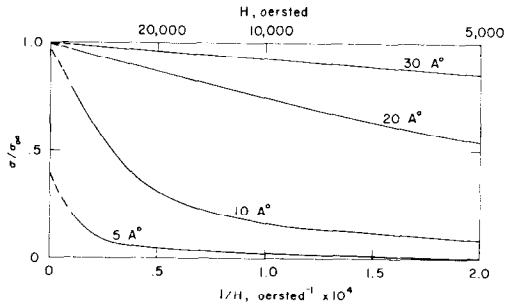

FIG. 2. $1/H$ plots for different sizes of nickel crystallites.

are possible. This approach is also limiting since crystallites above a critical value are no longer superparamagnetic at extremely low temperatures. Langevin curves must still be found at higher temperatures. Both saturation and superparamagnetism may be achieved with superconducting solenoid magnets, which gave fields up to 100 kOe.

Crystallite radii are readily calculated from magnetization curves such as those in Fig. 1 using low and high field approximations of the Langevin function (*9*). Thus

$$r_{\mathrm{LF}}^3 = \frac{9kT(\sigma/H)_{\mathrm{LF}}}{4\pi I_s \sigma_\infty}, \tag{2}$$

$$r_{\mathrm{HF}}^3 = \frac{3kT}{4\pi I_s H_{\mathrm{HF}}(1 - \sigma/\sigma_\infty)_{\mathrm{HF}}}. \tag{3}$$

If the specimen has only one size, then r_{LF} and r_{HF} are the same. Differences indicate a size distribution and r_{LF} is greater than r_{HF} since the larger crystallites are more readily magnetized at low fields. The task of extracting the distribution function from magnetization data is much more difficult.

For a crystallite size distribution, $f(r)$, the magnetization function is

$$\frac{\sigma(H)}{\sigma_\infty} = \int_0^\infty f(r)L(r, H)dr. \tag{4}$$

Reinen and Selwood (*11*) suggested that fitting experimental data to the expression

$$\frac{\sigma}{\sigma_\infty} = \sum_{n=1}^{\infty} D_n H^{2n-1}(-1)^{n+1}, \tag{5}$$

yields the series expansion of Eq. (4) with

$$D_n = \left(\frac{4\pi I_s}{3kT}\right)^{2n-1} \frac{2^{2n}}{(6n)!B_n} \frac{\overline{r^{6n}}}{\overline{r^3}}, \quad (6)$$

B_n is the Bernoulli coefficient and, in general,

$$\overline{r^m} = \frac{\int_0^\infty r^m f(r)dr}{\int_0^\infty f(r)dr}. \quad (7)$$

By comparing the coefficients from Eq. (5) with those calculated by Eq. (6) from trial distributions, it should be possible to deduce the type of distribution involved. Presumably the exact distribution parameters are then found from optimization with Eq. (4). This procedure is time-consuming with the possibility of ambiguous solutions. Furthermore, Eq. (5) converges only for $(I_s H 4\pi r^3/3kT) < \pi$ so that 50 Å crystallites may only be considered up to 12 kOe.

A more direct solution is to represent Eq. (4) by

$$\frac{\sigma(H)}{\sigma_\infty} = \sum_{n=0}^{\infty} g(n)L(n, H), \quad (8)$$

where n is a selected interval of r with $g(n)$ and $L(n, H)$ the respective average values of $f(r)$ and $L(r, H)$ over the interval.

The system of simultaneous equations

$$\begin{aligned}\left(\frac{\sigma}{\sigma_\infty}\right)_{H_1} &= g(r_1)L(r_1, H_1) \\ &\quad + g(r_2)L(r_2, H_1) + \cdots \\ \left(\frac{\sigma}{\sigma_\infty}\right)_{H_2} &= g(r_1)L(r_1, H_2) \\ &\quad + g(r_2)L(r_2, H_2) + \cdots \\ &\cdots\cdots\cdots\cdots\end{aligned} \quad (9)$$

need only be inverted to give the bar distribution $g(n)$.

This method has been used by Dreyer (*12*), but in practice experimental precision is such that round-off errors in matrix inversion methods limit the procedure to small orders. Inaccuracies associated with assuming average values of $L(n, H)$ then become significant and generally unreliable results are obtained.

Evdokimov and Kuznetsova *et al.* (*13*) derived the following expression from the thermodynamic relationships

$$r_H^3 = \frac{9kT(\sigma_H + \chi_H H)}{4\pi I_s H \sigma_\infty}, \quad (10)$$

where r_H is the radius of crystallites which saturate (i.e., have zero slope) at H. The fraction of the distribution with radii greater than r_H is the intercept of the tangent at H with the magnetization axis. The resulting cumulative distribution leads directly to the differential form. Calculations based on this procedure do not, however, give satisfactory results when applied to magnetizations calculated from known distributions. This may be due to the imprecision in measuring slopes and making extended extrapolations.

The most successful applications have been those of de Montgolfier and Martin (*14*) who assumed a distribution of the type

$$f(r) = e^{-ar} \sum_n b_n r^n. \quad (11)$$

Parameters were determined by optimization of calculated magnetization values with the experimental σ versus H curve. The constants of Eq. (11) include the weight fraction of metal in the sample so that σ_∞ need not be known. This method, although giving consistent results in some cases, generally suffers from the inherent limitations of too many adjustable parameters.

Many attempts have been made to find the distribution from the temperature dependence of the magnetization (*15, 16*) but all fail to provide satisfactory relationships

between crystallite size and ferromagnetic Curie points. Indeed, Abeledo and Selwood (*10*) find little dependence for crystallites above 15 Å radius.

Requirements for successfully calculating distribution curves from magnetic data are as follows: (a) Magnetization measurements should be made close to saturation. Either low temperatures or, preferably, high magnetic fields are necessary. Accurate extrapolations are then possible and the smaller crystals in the distribution are properly accounted for. (b) The sample should be confirmed superparamagnetic. Larger crystals may be ferromagnetic and invalidate the computations. Superposition of σ/σ_∞ vs H/T curves measured at different temperatures is indicative of superparamagnetic behavior. Tungler *et al.* (*17*) have outlined methods for treating mixed ferromagnetic and superparamagnetic systems. (c) The saturation magnetization must be known. This usually means extrapolation of σ vs $1/H$ data, for which near saturation data is needed. Carter and Sinfelt (*18*) sintered the sample at high temperatures after all other measurements were finished. The larger ferromagnetic crystals saturated easily. Satisfactory results are possible provided no gain or loss of reduced metal occurs, e.g., through surface oxidation, compound formation, etc. Alternatively, the amount of reduced metal could be measured by other means using chemical or instrumental procedures. This is acceptable only if *in situ* methods are used, since some loss of reduction may take place in sample handling. Evdokimov and Kuznetsova (*13*) have suggested another approach for finding σ_∞, but this has not proven reliable. (d) Since assumption of the type of distribution is not the most desirable situation, the best solution is inversion of the magnetization curve to give the required function directly. This is possible only if the data are accurate enough and the computational method allows a sufficiently high order or narrow interval. These methods are preferable over those involving slope analysis, which is usually far from precise.

A technique has been developed in this laboratory which involves elements of all of these. High field measurements are made with a superconducting solenoid. Superparamagnetism is confirmed with a low field Faraday apparatus at higher temperatures. An assumed distribution is adjusted to give an initial fit for a nonlinear inversion computation of the distribution histogram.

EXPERIMENTAL METHODS

Low Field Faraday Apparatus

The low field Faraday apparatus operated up to 8 kOe and consisted of a Model 4800 Alpha Scientific electromagnet with a Cahn No. 2000 RG electrobalance. A spherical silica bucket contained 50 mg of sample and was suspended into a flow-through hangdown tube in the inhomogeneous pole gap. The sample was dried at 200°C in helium and reduced at a standard condition with all weights recorded. Magnetization measurements were made up to 8 kOe over the temperature range 25–350°C, followed by measurements after sintering in helium at 700°C for 16 hr. These data were used to establish weight losses, to find σ_∞ and the degree of reduction, and to check superparamagnetism.

High Field Apparatus

The high field solenoid was a Magnion Incorporated Super-conducting Magnet with a high stability power supply. Although the solenoid operated at liquid helium temperatures, the room-temperature working volume was 5 cm in diameter with a field uniform within 3% over a length at 7.6 cm. Magnetic fields from 0 to 100 kOe were possible. Measuring coils fitted into this space, as shown schematically in Fig. 4. Each coil was 2 cm

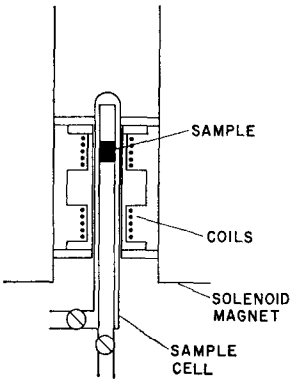

FIG. 4. High field solenoid pick-up coils.

in length, with three layers of No. 36 Formvar insulated wire for a total of 380 turns. They were connected in opposition 2 cm apart on a brass tube with an internal diameter of 1.3 cm. Plexiglass alignment plates were attached to the ends of the brass tube and the assembly was suspended from the top of the solenoid by an aluminum rod.

The sample cell contained the catalyst as shown. The outer tube was a 13 mm o.d. Vycor tube; the inner tube diameter was 7 mm. Sufficient sample was packed between quartz wool to give a bed length of 1–1.5 cm. Each tube was sealed with a high vacuum grade stopcock connected by 14/35 standard taper joints. With this arrangement the sample could be treated externally and reduced or sintered at desired conditions. Since the solenoid working volume was easily accessible during operation, many sample cells were prepared and run in sequence, thus improving economy and efficiency.

The sample cell was positioned with the catalyst in the center of the upper coil, then moved mechanically so that the catalyst shifted to the lower coil. A voltage, proportional to the magnetization of the sample and the coil geometry, was induced in the coils. This voltage pulse was measured with an oscilloscope (Hewlett-Packard Model 1200A Dual Trace) and recorded on film (Polaroid Type 107) using an oscilloscope camera (Hewlett-Packard Model 198A). The recorded signal was integrated to give the magnetization of the sample. Calibrations of instrumental constants were made with a sample of pure nickel powder. All measurements were at room temperature.

Surface Area Measurements

Hydrogen surface area measurements were made with a conventional volumetric adsorption apparatus equipped with a differential pressure capacitive manometer (MKS Baratron Type 1443-300). An advantage of the sample cell design was that the same sample measured in the solenoid could be used, although the dead volume correction was high with some sacrifice of accuracy.

Isotherms of hydrogen on the nickel, measured at 25°C, were flat after an initial fast adsorption. The area of the nickel atom was assumed to be 6.5 Å with a stoichiometry of one hydrogen per nickel atom.

Supported Nickel Catalysts

Two high level nickel catalysts were used—a precipitated 40 wt% Ni/SiO_2 (kieselguhr) and a coprecipitated 40 wt% Ni/Al_2O_3. Both catalysts had been calcined at 400°C and reduced for 12 hr in H_2 at 350°C. Specimens of the Ni/Al_2O_3 sample were also reduced for 36 and 72 hr to check the effect of reduction time.

Computation

The distribution coefficients, $g(r)$, were calculated using a subroutine BSOLVE (*19*) which solves n equations in k unknowns ($n \geq k$) by using Marquardts' adaptation of the Newton-Raphson method.

Equations (9) are rearranged as

$$y_1 = g(r_1)L(r_1, H_1) + g(r_2)L(r_2, H_1) + \cdots - \left(\frac{\sigma}{\sigma_\infty}\right)_{H_1},$$
$$y_2 = g(r_1)L(r_1, H_2) + g(r_2)L(r_2, H_2) + \cdots - \left(\frac{\sigma}{\sigma_\infty}\right)_{H_2}, \quad (12)$$
$$\cdots\cdots\cdots\cdots$$

Initial values for $g(r_1)$ $g(r_2)$, ..., $g(r_k)$ are provided to start the iterative search along the direction which minimizes

$$Q = y_1^2 + y_2^2 \cdots + y_n^2. \quad (13)$$

Since there may be more than one solution to Eqs. (9), the final solution is the closest to the initial set of values. Thus the choice of these becomes crucial.

Many crystallite size distributions examined by electron microscopy are skewed toward higher radii and have the general appearance of a log normal function (5). We selected this distribution as a "best" first guess for the computation.

The log normal function is

$$f(r) = \frac{1}{(2\pi)^{\frac{1}{2}} r \ln(\sigma)} \times \exp\left[-\left(\frac{\ln r - \ln r_0}{2^{\frac{1}{2}} \ln \sigma}\right)^2\right]. \quad (14)$$

There are only two parameters, r_0 and σ, which are conveniently related to the value of the n-th moment as follows

$$\overline{r^n} = \exp\left[n \ln (r_0) + \frac{n^2}{2} \ln^2 (\sigma)\right]. \quad (15)$$

For the low field approximation of the Langevin function

$$\left(\frac{\sigma}{\sigma_\infty}\right)_{LF} = \frac{4\pi I_s H}{9kT} \int_0^\infty f(r) r^3 dr, \quad (16)$$

so that

$$r_{LF}^3 = \overline{r^3}. \quad (17)$$

Similarly, for the high field approximation

$$\left(\frac{\sigma}{\sigma_\infty}\right)_{HF} = \int_0^\infty f(r) \times \left[1 - \frac{3kT}{4\pi I_s H_{HF} r^3}\right] dr, \quad (18)$$

and

$$r_{HF}^3 = 1/\overline{r^{-3}}. \quad (19)$$

Determination of r_{LF}^3 and r_{HF}^3 from magnetic data lead to $\overline{r^3}$ and $\overline{r^{-3}}$ from which the parameters, r_0 and σ, are found from Eq. (15).

In our computations, the experimental data were smoothed by fitting to one or several polynomial functions. Low and high field magnetizations at 500 and 90,000 Oe, respectively, were calculated from these functions and values of σ and r were found using Eqs. (2), (3), (15), (17), and (19). The initial set of $g(r)$ were calculated from the log normal distribution Eq. (14) and used to find the correct distribution with BSOLVE. The surface area of the assembly was calculated from

$$S = (6 \times 10^{-4})\overline{r^2}/(8.91\ \overline{r^3}) \ \text{m}^2/\text{g Ni}. \quad (20)$$

We checked the accuracy of these procedures with model distributions, one example of which is shown in Fig. 5, magnetic

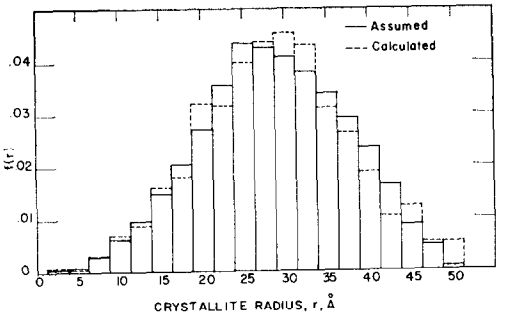

FIG. 5. Model crystallite size distribution with computed results.

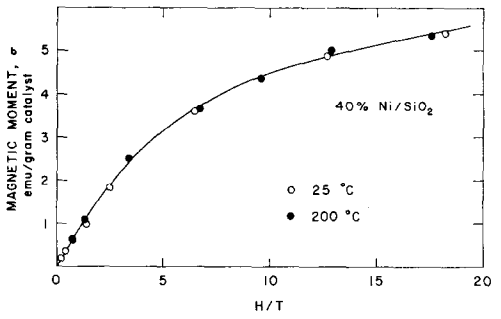

FIG. 6. Superposition of Langevin plots for 40% Ni/SiO_2.

data were calculated from the distributions and used as input to the program. The final results show that agreement is good when the distributions are normal or log normal but less quantitative, yet still qualitative, when the skew is toward lower radii. Since this situation is not common in real systems, the method is believed to be adequate in determining the distribution. Checks on bidisperse distributions were also very satisfactory.

RESULTS AND DISCUSSION

40 wt% Ni/SiO_2

Low field results at 25 and 200°C are plotted in Fig. 6 to demonstrate superposition of the H/T curve and the superparamagnetic behavior of the sample. In Fig. 7 both low and high field data are

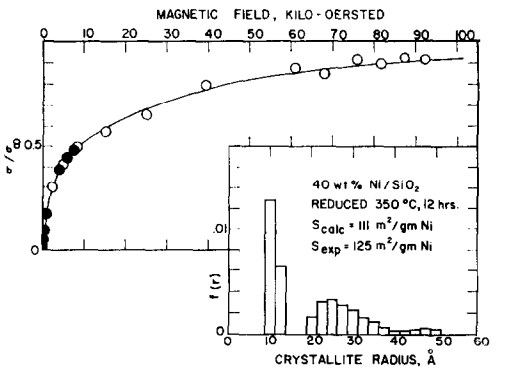

FIG. 7. Results for 40 wt% Ni/SiO_2.

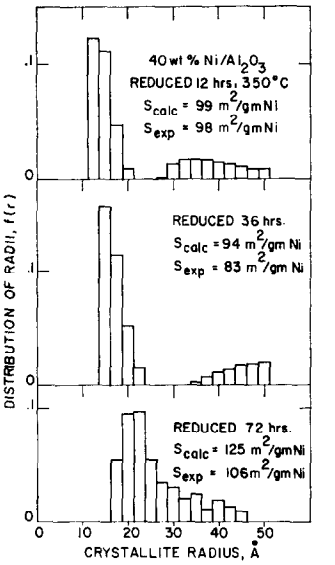

FIG. 8. Crystallite size distribution for 40 wt% Ni/Al_2O_3 reduced for 12, 36, and 72 hr.

shown. The two sets of data, measured and calibrated differently, fall on the same curve and support the consistency of the experimental procedures.

The saturation magnetization used in Fig. 7 was found from low field measurements on the sample after sintering at 800°C. This value, 20.8 emu/g cat was in excellent agreement with the high field result, 21.0 emu/g cat which was determined from the linear extrapolation of the $1/H$ plot. We infer from this that saturation magnetizations of the small crystallites are independent of size, a conclusion that has been accepted by many authors.

These magnetic data were processed with the computational program discussed above and the resulting crystallite size distribution is given in Fig. 7. The curve drawn through the experimental points was calculated from the distribution. Also compared are the calculated and experimental surface areas, which show very good agreement.

The distribution itself is bidisperse. Qualitatively, this result is suggested by the shape of the magnetization curve. We

cannot comment further on the reasons for the bidisperse distribution except to speculate that metal–support compound formation (e.g., nickel silicates) or the pore structure of the support may play a role.

40 wt% Ni/Al_2O_3

Histograms for the three samples reduced for 12, 36, and 72 hr, respectively, are shown in Fig. 8. Supporting magnetic data—Langevin plots, low and high field agreement, etc.—were as good as the previous example and are not repeated.

The measured distributions demonstrate the usefulness of this method in the measurement of sintering phenomena. Initially, the distribution is bidisperse and may originate from the reduction of both NiO and $NiAl_2O_4$ formed during calcining. We speculate that the large crystallites originate from the NiO and the smaller distribution from $NiAl_2O_4$. Only 38% of the available nickel had been reduced in this time.

Longer periods resulted in 50% reduction of the nickel but with an upward shift of the distribution. Finally, after 72 hr, no further nickel reduction had occurred but the two distributions now overlap into a log normal type.

Ruckenstein and Pulvermacher (*2*) have advanced a sintering model which involves the migration of small crystallites across the support. Wynblatt and Gjostein (*4*) suggested that this mechanism is limited to crystallites 25 Å radius or smaller and that larger particles sinter via the interparticle transport model favored by Flynn and Wanke (*3*). The results in Fig. 8 tend to favor the crystallite migration model for those radii below 25 Å. The peak of the distribution moves upward, the distribution does not broaden with the generation of smaller crystallites necessitated by interparticle transport. The large crystallites, however, merge into the lower distribution. This is possibly a manifestation of material transfer predicted for this size range. Although these results are to be expected for concentrations this large, the data are too preliminary to be conclusive. Furthermore, support morphology may be important in directing the course of the process (*4*). Much more work will be necessary in order to resolve these points.

CONCLUSIONS

Experimental and computational methods have been developed for the calculation of crystallite size distributions from magnetization curves. These techniques overcome many past objections and have been successfully demonstrated as both model and real dispersed systems. Initial results indicate a potential for the method in the study of sintering phenomena.

ACKNOWLEDGMENTS

We are grateful to the Robert A. Welch Foundation for continued support of this project. Experimental results are taken, in part, from the theses of J. E. Rosser (*20*) and L. R. Vincent (*21*). The assistance of Professor W. I. Honeywell in conducting high field measurements was invaluable.

REFERENCES

1. Luss, D., *J. Catal.* **23**, 119 (1971).
2. Ruckenstein, E., and Pulvermacher, B., *AIChE J.* **19**, 224, 356 (1973).
3. Flynn, P. C., and Wanke, S. E., *J. Catal.* **34**, 390, 400 (1974).
4. Wynblatt, P., and Gjostein, A., *Prog. Solid State Chem.* **9**, 21 (1975).
5. Adams, C. R., Benesi, H. A., Curtis, R. M., and Meisenheimer, R. G., *J. Catal.* **1**, 336 (1962).
6. Whyte, T. E., Jr., Kirklin, P. W., Gould, R. W., and Heinemann, H., *J. Catal.* **25**, 407 (1972).
7. Flynn, P. C., Wanke, S. E., and Turner, P. S., *J. Catal.* **33**, 233 (1974).
8. Bean, C. P., and Jacobs, I. S., *J. Appl. Phys.* **27**, 1448 (1956).
9. Selwood, P. W., "Adsorption and Collective Paramagnetism." Academic Press, New York, 1962.
10. Albedo, C. R., and Selwood, P. W., *J. Appl. Phys.* **32**, 229 (1961).
11. Reinen, D., and Selwood, P. W., *J. Catal.* **2**, 109 (1963).

12. Dreyer, H., *Z. Anorg. Allg. Chem.* **362,** 233 (1968).
13. Evdokimov, V. B. E., and Kuznetsova, M. N., *Russ. J. Phys. Chem.* **44,** 1435 (1970).
14. De Montgolfier, P., and Martin, G. A., *C. R. Acad. Sci., Ser. C* **273,** 1209 (1971).
15. Selwood, P. W., Adler, S., and Phillips, T. R., *J. Amer. Chem. Soc.* **77,** 1452 (1955).
16. Evdokimov, V. B., and Kuznetsova, M. N., *Russ. J. Phys. Chem.* **44,** 1742 (1970).
17. Tungler, A., Petró, J., Mathé, T., Csurös, A., and Lugosi, K., *Acta Chim. Acad. Sci. Hung.* **79,** 289 (1973).
18. Carter, J. L., and Sinfelt, J. H., *J. Catal.* **10,** 134 (1968).
19. Henley, E. J., and Rosen, E. M., "Material and Energy Balance Computations." Wiley, New York, 1969.
20. Rosser, J. E., "Magnetic Studies in Dispersion Effects in Reduced Nickel Catalysts." M.S. Thesis, Dept. Chem. Eng., Univ. of Houston, 1972.
21. Vincent, L. R., "High Magnetic Field Measurements of Nickel Crystallite Size Distributions." M.S. Thesis, Dept. Chem. Eng., Univ. of Houston, 1973.